NACA RM E53K04

6850

NACA

RESEARCH MEMORANDUM

ANALYTICAL AND EXPERIMENTAL STUDIES OF A

DIVIDED-FLOW RAM-JET COMBUSTOR

By E. E. Dangle, Robert Friedman, and A. J. Cervenka

Lewis Flight Propulsion Laboratory
Cleveland, Ohio

NATIONAL ADVISORY COMMITTEE
FOR AERONAUTICS
WASHINGTON
January 11, 1954

NATIONAL ADVISORY COMMITTEE FOR AERONAUTICS

RESEARCH MEMORANDUM

ANALYTICAL AND EXPERIMENTAL STUDIES OF A

DIVIDED-FLOW RAM-JET COMBUSTOR

By E. E. Dangle, Robert Friedman, and A. J. Cervenka

SUMMARY

An analytical evaluation and an experimental investigation of a divided-flow ram-jet combustor compared with a nondivided-flow combustor are presented in this report. The analytical evaluation demonstrated the increase in the total-pressure ratio across the combustor with increase in the primary-zone area. With proper selection of the primary-zone area, the divided-flow combustor exhibits improved total-pressure ratios over the corresponding nondivided-flow combustor even with higher flame-holder pressure-loss coefficients in the divided-flow case.

The experimental investigation demonstrated that a divided-flow combustor had higher combustion efficiencies than a nondivided-flow combustor over a range of fuel-air ratios from 0.011 to 0.034. At a fuel-air ratio of 0.017, the efficiency of the divided-flow combustor was 98 percent while that of the nondivided-flow combustor was approximately 70 percent. The ratio of combustor-outlet total pressure to combustor-inlet total pressure was approximately 0.95 over a range of engine total-temperature ratios of 1.6 to 3.0 and was equal for both the divided- and nondivided-flow combustors. The experimental investigations were conducted in a 16-inch-connected-pipe ram-jet engine.

INTRODUCTION

The investigation reported herein is a continuation of a ram-jet-combustor design program being conducted at the NACA Lewis laboratory. The purpose of this broad program is to establish basic design criteria for combustors operating over wide ranges of fuel-air ratio with low pressure losses and high combustion efficiency, and to utilize these design criteria in the development of practical ram-jet combustors.

It is generally accepted that the most efficient burning in a ram-jet combustor occurs in regions of low velocity and near stoichiometric fuel-air ratios. In most burners, this condition is created locally in

the low-velocity region behind flame-holder baffles. However, relying on baffles alone to create a sheltered zone where burning may be completed is not entirely satisfactory. Mixing with high-velocity air often occurs before combustion is firmly established; local fuel-air ratios cannot be easily controlled; and all the air stream is subjected to momentum pressure losses in the combustor, whereas actually only a portion of the air enters into the reaction at over-all lean fuel-air ratios.

A possible improvement in combustor design is offered in the form of a divided-flow system, in which a portion of the combustor air is ducted by a sleeve into an inner or primary zone of low-velocity burning while the remainder or secondary air passes around the sleeve. The two streams then mix downstream of the primary combustion zone. Evidence of improved combustion performance through the use of a flow-dividing sleeve is given in references 1 and 2, in which high combustion efficiency was achieved over a wide range of fuel-air ratios. This achievement was a result of better control of the fuel-air ratio provided by the sleeve. Similarly, the existence of a low-velocity burning zone offers further improvements in combustion efficiency as shown by a correlation of burner velocity with pressure and temperature presented in reference 3. Finally, the low burner velocity of the divided-flow system makes it possible to utilize high-blockage flame holders in the combustor without reducing the total-pressure ratio across the engine. The advantages associated with the divided-flow combustor are dependent upon achieving a low approach velocity to the primary zone by means of proper proportioning of primary-zone area and air flow. The objectives of this report, therefore, are to present an analytical study on the influence of primary-zone area and air mass flow upon the pressures throughout a ram-jet combustor; to establish an optimum combustor design in terms of reduced pressure losses; and to evaluate experimentally a representative combustor evolved from the analysis.

Pressures throughout a turbojet combustor are analyzed in reference 4 by the use of incompressible-flow relations. However, in this investigation the diffusion, combustion, and mixing processes are determined by one-dimensional compressible-flow relations so that the total-pressure losses can be determined for the case of high inlet-air velocities such as occur in the ram-jet combustor. Evaluation of the pressure losses through the divided-flow system is based upon the flight conditions, and the pressure losses are compared with corresponding losses in the nondivided-flow combustor.

Experimental evaluation of the combustor performance was conducted in a 16-inch-connected-pipe ram-jet engine at conditions simulating a flight Mach number of 2.9 and altitude of 67,000 feet. Efforts were limited to evaluation of the combustion efficiency, the pressure recovery, and the mechanical reliability of the burner, while no efforts were made to refine the operational characteristics.

3042

SYMBOLS

The following symbols are used in this report:

A   cross-sectional area, sq ft

C_D flame-holder pressure-loss coefficient, $\dfrac{P_2-P_3}{q_2}$

c   specific heat, Btu/(lb mass)(^{O}R)

g_c conversion factor between force and mass units, 32.2 $\dfrac{\text{(lb mass)(ft)}}{\text{(lb force)(sec}^2)}$

M   Mach number

P   total, or stagnation, absolute pressure, lb force/sq ft

p   static absolute pressure, lb force/sq ft

q   dynamic pressure, $1/2\ p\gamma M^2$, lb force/sq ft

R   gas constant per unit mass, (ft-lb force)/(lb mass)(^{O}R)

T   total, or stagnation, absolute temperature, ^{O}R

t   static absolute temperature, ^{O}R

v   linear velocity, ft/sec

W   mass-flow rate, lb mass/sec

γ specific-heat ratio

η_D diffuser efficiency, P_2/P_0

τ total-temperature ratio across combustor

Subscripts:

A,B,C   any generalized engine stations

ref   reference value for heat balance

0,1,2,2a,
2b, . . .   stations in analytical engine models, fig. 1

ANALYSIS

Description of Idealized Engine

As the advantages of the divided-flow combustor with regard to improved combustion efficiency and flame stability are well recognized, this analysis is concerned only with the proper apportioning of the primary-zone and secondary-zone flow areas. The evaluation of the divided-flow system is made through calculation of the ratio of combustor-outlet total pressure to free-stream total pressure, referred to herein as the total-pressure ratio. The desired flow areas, therefore, would be those in which the total-pressure ratio would equal or exceed that of a corresponding nondivided-flow system of the more conventional type, for the same average temperature ratio across the combustor.

The divided-flow system, illustrated in figure 1(a), consists of a supersonic and subsonic diffuser, stations 0 to 2, the divided combustion zone, stations 2 to 5, and the mixing region before the exit nozzle, stations 5 to 6. In the primary zone, the flame holder is situated between stations 2a and 3a, and stoichiometric burning takes place between stations 3a and 4a. The secondary-zone air passes from station 2b to 5b unchanged. At stations 5a and 5b a nozzle is introduced, either converging or diverging as required, to balance the primary- and secondary-stream static pressures. In this way, the primary-zone air flow is kept independent of the primary-combustor-zone area. Mixing of the primary and secondary streams occurs between stations 5 and 6; and, if additional over-all temperature ratio is desired, secondary-stream fuel injection and burning may be provided in regions 5 to 6. Figure 1(b) shows a conventional nondivided-flow configuration in which combustion occurs between stations 3 to 6, resulting in a temperature ratio equivalent to that between stations 3a to 6 in the divided-flow combustor.

Method of Analysis

Schematically, an example of the variations of total-pressure ratio through the divided-flow and the comparable nondivided-flow systems is shown in figure 2. The plot shows the ratio of total pressure at each station to the free-stream total pressure and illustrates the design requirements of the divided-flow system. The primary-zone area selected is large enough to ensure a low-velocity combustion region between stations 3a and 4a which results in smaller pressure losses than in the nondivided-flow system. On the other hand, the secondary-zone area is not reduced to such an extent that skin-friction losses in the secondary zone between stations 2b and 5b are appreciable. The analytical engine model is considered as a series of successive flow-path steps. At each step the gas streams undergo a single operation or simple change, and new values of

flow properties are calculated for the simple change. The over-all change in conditions is the summation of these individual changes.

The following assumptions are made for the analytical model:

(1) The flows may be considered one dimensional.

(2) Heat loss, skin friction, and momentum effects of fuel addition are negligible except where noted.

(3) In the divided-flow system, combustion takes place in the primary zone only, stations 3a to 4a, at 100 percent efficiency, and there is no heat transfer between streams until the mixing zone, between stations 5 and 6.

(4) In the divided-flow system, mixing of the two streams is complete and temperature equilibrium is established by station 6.

The gas streams in both idealized engines are subjected to these possible simple changes:

(1) Isentropic area change

(2) Constant-area temperature change

(3) Change associated with flow through a flame holder at an assumed pressure-loss coefficient

(4) Constant momentum mixing

The following one-dimensional equations, written for variable specific-heat ratios, relate the changes of properties for these operations:

Area change (ref. 5 and pp. 139-147 of ref. 6):

$$A_B = A_A \frac{M_A}{M_B} \left[\frac{2\left(1 + \frac{\gamma_B - 1}{2} M_B^2\right)}{\gamma_B + 1} \right]^{\frac{\gamma_B+1}{2(\gamma_B-1)}} \left[\frac{\gamma_A + 1}{2\left(1 + \frac{\gamma_A - 1}{2} M_A^2\right)} \right]^{\frac{\gamma_A+1}{2(\gamma_A-1)}} \eta_D$$

$$(1)$$

$$p_B = p_A \left[\frac{\gamma_B + 1}{2\left(1 + \frac{\gamma_B - 1}{2} M_B^2\right)} \right]^{\frac{\gamma_B}{\gamma_B - 1}} \left[\frac{2\left(1 + \frac{\gamma_A - 1}{2} M_A^2\right)}{\gamma_A + 1} \right]^{\frac{\gamma_A}{\gamma_A - 1}} \eta_D \quad (2)$$

The subscripts A and B denote values of the properties at stations immediately before and after the change. When the area change is isentropic, the diffuser efficiency η_D is equal to 1.

Temperature change (ref. 5 and pp. 148-156 of ref. 6):

$$T_B = T_A \frac{(M_B)^2 (\gamma_B + 1)\left(1 + \frac{\gamma_B - 1}{2} M_B^2\right)\left(1 + \gamma_A M_A^2\right)^2}{(M_A)^2 (\gamma_A + 1)\left(1 + \frac{\gamma_A - 1}{2} M_A^2\right)\left(1 + \gamma_B M_B^2\right)^2} \quad (3)$$

$$p_B = p_A \frac{(1 + \gamma_A M_A^2)(\gamma_B + 1)}{(1 + \gamma_B M_B^2)(\gamma_A + 1)} \quad (4)$$

Flame-holder static-pressure loss (derived in appendix A):

$$p_B = p_A \frac{\left(1 + \frac{\gamma_A - 1}{2} M_A^2\right)^{\frac{\gamma_A}{\gamma_A - 1}} - \frac{1}{2} \gamma_A M_A^2 C_D}{\left(1 + \frac{\gamma_B - 1}{2} M_B^2\right)^{\frac{\gamma_B}{\gamma_B - 1}}} \quad (5)$$

$$M_B = M_A \frac{p_A}{p_B} \frac{A_A}{A_B} \sqrt{\frac{\gamma_A t_B}{\gamma_B t_A}} \quad (6)$$

Mixing (derived in appendix B):

$$t_C = t_B + \frac{(t_A - t_B) c_A W_A}{c_C W_C} \quad (7)$$

3042

$$P_C = P_B \frac{A_A M_A \sqrt{\frac{\gamma_A}{R_A t_A}} + A_B M_B \sqrt{\frac{\gamma_B}{R_B t_B}}}{A_C M_C \sqrt{\frac{\gamma_C}{R_C t_C}}} \tag{8}$$

$$M_C = \sqrt{\left(\frac{P_B}{P_C}\right)\left(\frac{A_A(1 + \gamma_A M_A^2) + A_B(1 + \gamma_B M_B^2)}{A_C \gamma_C}\right) - \frac{1}{\gamma_C}} \tag{9}$$

The subscripts A and B denote the values of the properties of the two streams before mixing and C, the values of the properties of the mixed stream.

The total (or stagnation) temperature and pressure relations, equations (10) and (11), complete the necessary equations for the stepwise calculations:

$$P = p\left(1 + \frac{\gamma - 1}{2} M^2\right)^{\frac{\gamma}{\gamma - 1}} \tag{10}$$

$$T = t\left(1 + \frac{\gamma - 1}{2} M^2\right) \tag{11}$$

The application of equations (1) to (11) to the calculation of the total-pressure change in a divided-flow configuration is shown in appendix C. A sample calculation is included for both a divided-flow design and a comparable nondivided-flow system.

Conditions for Analysis

The analysis presented is general for any case in which the combustor-inlet Mach number M_2 is equal to 0.18, and the heat addition occurs equivalent to the values listed subsequently.

A typical set of engine and flight conditions that correspond to the general analysis has been selected for the purpose of illustrating the analysis and is presented as follows:

Free-stream Mach number 3.0
Inlet total temperature, °R 1100
Supersonic-diffuser efficiency, percent 65
Subsonic-diffuser efficiency, percent 100
Ratio of combustor-inlet area to free-stream capture area 1.2
Hydrogen-carbon mass ratio of fuel 0.167
Stoichiometric fuel-air ratio 0.067
Total-temperature ratio across primary combustion zone 4.05
Flame-holder pressure-loss coefficient, $\Delta P/q$ . . . . 2 and 10

In the definition of the pressure-loss coefficient, ΔP is the total-
pressure drop across the flame holder with cold flow and q is the
dynamic pressure in the primary stream immediately before the flame
holder. For the analysis, the diffuser throat is assumed choked at all
times.

Provision for the variable total-temperature ratios τ across the
engine is made by the selection of five primary-zone air flows of 20,
25, 30, 35, and 40 percent of the total engine air flow.

ANALYTICAL RESULTS

Pressure Recovery

In figure 3 is shown the effect of the size of the primary combustor
area upon the over-all pressure recovery P_6/P_0 for a single operating
condition of 25-percent primary-zone air flow. The plot shows the
pressure-recovery curves for two cases of flame-holder pressure-loss
coefficients $\Delta P/q$ of 2 and 10. For comparison, the pressure recovery
of a nondivided-flow combustor for the same over-all fuel-air ratio and
$\Delta P/q$ of 2 is shown by a horizontal line, although the abscissa values
of primary-zone area would have no meaning for this case.

It is evident from figure 3 that the pressure recovery of the
divided-flow system increases with increasing primary-zone area and
can be made to exceed that of a conventional nondivided-zone configu-
ration by the use of a large primary-zone area. The maximum primary-
zone area is limited to a size where secondary-stream Mach numbers are
not excessive. Preliminary calculations showed that above a secondary-
stream Mach number of 0.7, the secondary skin-friction losses become
appreciable. Thus the curve in figure 3 is extended only up to a
primary-zone area of 75 percent of the total combustor area, at which
point the secondary-stream Mach number is 0.7.

The curves of total-pressure ratio for primary-zone air flows of 20
to 40 percent are shown in figure 4(a) for a flame-holder pressure-loss

3042

coefficient of 2 and in figure 4(b) for a flame-holder pressure-loss coefficient of 10. The effect of primary-zone area is shown in the figures. The broken line indicates the corresponding values of the conventional nondivided-flow systems for the same total-temperature ratios across the combustors. All the curves are extended up to an area ratio where the secondary-zone Mach number is 0.7.

From figure 4 it may be seen that it is possible to exceed the total-pressure ratio of the corresponding nondivided-flow configuration by an appropriate choice of primary-zone area. For example, with 25-percent air flow through the primary zone, improved pressure recovery over the conventional design is realized by utilizing primary-zone areas ranging from 30 to 75 percent of the total combustor area for a flame-holder pressure-loss coefficient of 2 and from 48 to 75 percent of the total area for a coefficient of 10. The curves for flame-holder pressure-loss coefficients of 10 show that the divided-flow system can tolerate a high-blockage flame holder and still equal or better the total-pressure recovery of a conventional system with a flame-holder pressure-loss coefficient of only 2.

Outlet Nozzle of Divided-Flow Combustor

The area of the nozzle at station 5 necessary for equalizing the static pressures at stations 5a and 5b is shown in figure 5(a) for a flame-holder pressure-loss coefficient of 2 and in figure 5(b) for a coefficient of 10. The size of the exit is plotted as a function of the primary-zone area for the range of primary-zone air flows considered in this analysis.

A broken line is drawn in figure 5 connecting points where the required exit area is the same as the primary-zone area. At all points above and to the left of this broken line, a diverging combustor exit nozzle is required; at all points below and to the right of this line, a converging nozzle is required. Intersection of the dashed line with the curves represents a condition where no exit nozzle is required.

Application to Design

A divided-flow combustor was designed for long-range missile application. The over-all engine fuel-air ratio was established at approximately 0.02 for the most efficient cruise phase and near stoichiometric fuel-air ratios for acceleration and climb. With primary-zone air flow at 25 percent of the total engine air flow and stoichiometric burning in the primary zone, the engine over-all fuel-air ratio resolved to 0.017 with gasoline fuel.

From figure 3 it is shown that with a flame-holder pressure-loss coefficient of 2 any primary-zone area between 30 and 75 percent of the total engine area could be selected for a practical combustor design. A primary-zone area of 50 percent was chosen. Again, from figure 3, it is seen that for the case of a combustor with a 50-percent primary-zone area, any flame-holder pressure-loss coefficient between 2 and 10 would result in reduced total-pressure losses as compared with those of a conventional engine.

APPARATUS AND EXPERIMENTAL PROCEDURE

The tests for this program were conducted in a 16-inch-connected-pipe ram-jet engine, the installation and details of which are given in reference 2. Sketches of the engine and engine installation are shown in figure 6.

Flame holders. - A sloping-baffle flame holder was utilized in the divided-flow system in the primary combustor and was installed as shown in figure 7. The flame holder consisted of nine radial V-gutters with a blocked area of 65 percent based on maximum primary-zone cross-sectional area. The downstream open end of the gutters tapered from $2\frac{1}{4}$ inches across at the outer diameter of the flame holder to $1\frac{3}{8}$ inches at the inner diameter. The flame holder extended from the centerbody pilot to the flow-divider sleeve at an angle of 20° to the engine axis. The flame-holder pressure-loss coefficient was 5.2 based on a measured static differential pressure across the flame holder converted to total pressure, and a dynamic pressure calculated from the primary-stream area, the static pressure, and the primary-zone air flow. The flame holder used in the nondivided-flow combustor had a pressure-loss coefficient of 1.5 and is described in detail in reference 1.

Air flow divider. - Installation of the flow-dividing sleeve in the ram-jet combustor is also shown in figure 7. The sleeve tapered from an inlet diameter of $10\frac{3}{16}$ inches to a diameter at the flame holder of $11\frac{3}{16}$ inches. The sleeve was 25 inches long, 20 inches of which were tapered and 5 inches of which had a constant diameter downstream of the flame holder. The sleeve cross-sectional area occupied 50 percent of the total engine cross-sectional area.

Fuel injection systems. - Fuel was injected into the primary fuel zone through six spray bars, each with a 0.0469-inch-diameter orifice located on the downstream side of the spray bar. The spray bars were located $16\frac{1}{2}$ inches upstream of the pilot-burner exit with the orifices located midway across the annulus between centerbody and inlet lip of the flow-divider sleeve.

3042

CH-2 back

Fuel was sprayed into the outer or secondary zone through 16 modified fixed-area commercial nozzles rated at 0.36 gallon per minute each at a pressure differential of 100 pounds per square inch. The nozzles were located 17 inches upstream of the flame holder.

It should be noted at this time that if the experimental combustor were to comply with the analytical model, the flow-dividing sleeve should diverge at the exit to an area corresponding to 64 percent of the engine area as interpolated between figures 5(a) and (b). However, since the fuel supply manifolds to the 16 nozzles already blocked a portion of the secondary-stream flow area, the diverging exit to the sleeve was disregarded.

Instrumentation. - The diffuser-exit velocity profile was established from readings taken from three total-pressure rakes equally spaced around the diffuser exit. Static-pressure taps were located along the inner surface of the flow-dividing sleeve at the inlet lip and before and after the flame holder. A radially movable total-pressure probe was located just upstream of the flame holder in the annulus formed by the sleeve and the outer wall. A water-cooled total-pressure probe was located at the combustor exit and was capable of making complete radial traverses from combustor wall to wall.

Fuel. - The specifications and analytical data on MIL-F-5624A grade JP-4 fuel used in this test program are presented in table I.

Combustor operating conditions. - The combustor operating conditions are:

Inlet-air static pressures, in. Hg abs 32-36
Inlet-air total temperature, $^{\circ}$F . . . . 600±10
Inlet-air velocities, ft/sec 230-260

These values correspond to the combustor-inlet conditions in a ram-jet engine flying at a Mach number of 2.9 at an approximate altitude of 67,000 feet with a diffuser pressure recovery of 65 percent.

Combustion efficiency. - Combustion efficiencies were determined by a heat-balance system similar to the system presented in reference 7. The quench-water mass flow was varied so that an average outlet temperature of 900° F was maintained. The total enthalpy change of fuel, air, quench water, and engine cooling water was divided by the input energy of the fuel to obtain the combustion efficiency. Operation of the engine was confined to a maximum fuel-air ratio of 0.043 because of limitations in the calorimeter.

EXPERIMENTAL RESULTS AND DISCUSSION

Combustion Efficiency

The effect of primary-stream fuel-air ratio upon combustion efficiency in the primary burner is shown in figure 8. The maximum combustion efficiency of 98 percent occurred at a primary-stream fuel-air ratio of 0.067, which corresponds to the design fuel-air ratio used in the analytical treatment. The fuel-air ratios employed in figure 8 were based upon a 25-percent primary-zone air flow. Varying the primary-stream fuel-air ratio over the range from 0.045 to 0.134 resulted in maximum-to-minimum combustion-efficiency variations of 98 to 82 percent. Combustion efficiency of 92 percent at a primary-stream fuel-air ratio of 0.134 would indicate that either secondary air recirculates into the primary zone or that primary-zone burning is not completed inside the primary zone but is completed with the aid of secondary air downstream of the primary zone. Figure 8 also indicates the effectiveness of a large primary-zone burner for a ram-jet engine operating at lean over-all fuel-air ratios. Between over-all fuel-air ratios of 0.015 to 0.034, the combustion efficiency varied from 98 to 90 percent, while at a fuel-air ratio of 0.011, the efficiency was 82 percent.

A plot of combustion-efficiency variation with engine over-all fuel-air ratio for primary-stream fuel injection and primary- plus secondary-stream fuel injection is presented in figure 9. For the cases of secondary-stream fuel injection, the primary-stream fuel-air ratio was held constant at 0.017 and 0.023 based on engine air flow and 0.067 to 0.092 based on primary-zone air flow, while the secondary-stream fuel flow was varied over a range of over-all fuel-air ratios from 0.025 to 0.043. It is seen, from the figure, that there is negligible effect on the over-all combustion efficiency with the above variation in primary-stream fuel-air ratio.

The lower combustion-efficiency level, 81 to 90 percent between fuel-air ratios of 0.026 to 0.043, associated with secondary-stream fuel injection is primarily due to the absence of secondary-stream flame-holding surfaces without the aid of which the secondary fuel-air stream must ignite by mixing with the hot primary exhaust stream. For this combustor operating over a range of fuel-air ratios from 0.011 to 0.034, primary-stream fuel injection alone appears most desirable.

The combustion-efficiency curve for a nondivided-flow combustor which was tested under similar conditions (ref. 1) is included in figure 9 for comparison with the divided-flow combustor. The divided-flow-combustor efficiency, with primary-zone burning only, is 28 percentage points higher than the nondivided-flow combustor at a fuel-air ratio of 0.017, while at a fuel-air ratio of 0.034 the combustion efficiencies are nearly equal. It is seen that with primary-zone combustion only, the divided-flow combustor is more efficient than the nondivided-flow combustor up to a fuel-

3042

air ratio of 0.034. With secondary-stream fuel injection, however, the efficiency of the divided-flow combustor is less than that of the nondivided-flow combustor (8 percentage points at a fuel-air ratio of 0.030 and 4 points at a ratio of 0.038). It is reasonable to assume that the efficiencies of the divided-flow combustor would be improved by the use of secondary-stream flame holders.

Total-Pressure Ratio

Variation in the ratio of combustor-outlet total pressure to combustor-inlet total pressure P_6/P_2 as a function of the combustor total-temperature ratio τ is presented in figure 10 for both the divided- and nondivided-flow combustors. From the figure, it is seen that the total-pressure losses for both systems are comparable. The ratio P_6/P_2 remained nearly constant at about 0.95 over a range of τ from approximately 1.6 to 3.0 for both systems.

It is of interest to compare the analytical predictions for total-pressure ratios across the two types of combustors with the experimental values obtained. The analytical method of this report (fig. 3) predicts a total-pressure ratio of 0.608 for a divided-flow combustor of 50-percent primary area, 25-percent primary-zone air flow, a flame-holder pressure-loss coefficient of 5 (by interpolation), and a 65-percent diffuser recovery factor which, when adjusted to a value of 100-percent diffuser recovery, gives a total-pressure ratio of 0.935. The total-pressure ratio for the analytical model of the nondivided-flow combustor was 0.603, which, when corrected for 100-percent diffuser recovery, was 0.928. This total-pressure ratio for the nondivided-flow combustor was calculated for a flame-holder pressure-loss coefficient of 1.5 instead of 2 as presented in the analytical treatment. The experimental total-pressure ratios in the connected-pipe installation were 0.953 with 100-percent diffuser recovery for both the divided- and nondivided-flow combustors at an over-all fuel-air ratio, corresponding to that of the analytical model of 0.017. The experimental data, which prove that the total-pressure ratios for the two systems are equal, bear out the predicted agreement between the two systems from the analytical treatment (0.935 for the divided-flow combustor and 0.928 for the nondivided-flow combustor) Exact quantitative agreement between the analytical and experimental methods was not achieved perhaps because of differences in the combustor-inlet Mach numbers for the two methods (0.15 for the experimental method and 0.18 for the analytical method).

Mechanical Reliability

The flow-dividing sleeve and the flame holder remained undamaged after 50 hours of operation with over-all fuel-air ratios as rich as 0.043.

SUMMARY OF RESULTS

The following results were obtained from a theoretical analysis and an experimental investigation of a divided-flow and a nondivided-flow combustor.

The following results were established from the theoretical analysis:

1. The total-pressure ratio of a divided-flow combustor increased with increasing primary-zone area. The maximum primary-zone area was limited only by friction losses in the secondary zone which became significant above secondary-zone Mach numbers of 0.7.

2. With the proper selection of primary-zone area in a divided-flow combustor, it was possible to exceed the total-pressure ratio of a nondivided-flow combustor.

3. It was possible to tolerate higher flame-holder pressure-loss coefficients in a divided-flow system than in a nondivided-flow combustor and still maintain a higher total-pressure ratio.

The following results were obtained from the experimental investigation conducted in a 16-inch ram-jet engine:

1. Operation at the selected design conditions of stoichiometric burning in the primary zone at a primary-zone air flow of 25 percent of the total engine air flow and a sleeve area of 50 percent of the engine area resulted in a combustion efficiency of 98 percent. This efficiency occurred at an over-all engine fuel-air ratio of 0.017.

2. The divided-flow system showed substantial gains in combustion efficiency at lean fuel-air ratios (0.011 to 0.034) over a conventional nondivided-flow combustor. At a fuel-air ratio of 0.017, the efficiency of the divided-flow combustor was 98 percent, while that of the nondivided-flow combustor was approximately 70 percent.

3. The ratio of total pressure at the combustor outlet to total pressure at the combustor inlet P_6/P_2 was equal for both the divided-flow and the nondivided-flow combustors, although flame-holder pressure-loss coefficients were 5.2 and 1.5, respectively. Over a range of engine total-temperature ratio τ from 1.6 to 3.0, the pressure ratio P_6/P_2 remained constant at approximately 0.95.

4. The flow-dividing sleeve and flame holder remained undamaged after 50 hours of operation with over-all fuel-air ratios up to 0.043.

CONCLUDING REMARKS

The divided-flow combustor has certain advantages over the nondivided-flow combustor. Increased efficiencies at lean fuel-air ratios were made possible by the low velocity flow in the relatively large primary zone of the divided-flow combustor. The divided-flow combustor can tolerate higher-blockage flame holders than the nondivided-flow combustor with no sacrifice in total-pressure ratio. Finally, the fact that a large portion of the engine area and only a small portion of the engine air can be utilized in the primary zone without loss in total-pressure ratio was shown by the theoretical analysis and the experimental evaluation.

Lewis Flight Propulsion Laboratory
    National Advisory Committee for Aeronautics
        Cleveland, Ohio, November 9, 1953

APPENDIX A

DERIVATION OF FLAME-HOLDER LOSS RELATIONS

The total-pressure losses across the flame holder are expressed by the pressure-loss coefficient C_D, which is defined as

$$C_D = \frac{\Delta P}{q} = \frac{P_A - P_B}{q_A} \tag{A1}$$

where station A is before the flame holder and B is after the flame holder. In this work, the dynamic pressure q in the definition of the pressure-loss coefficient is always taken as the value at the station just before the flame holder.

Total pressure and dynamic pressure may be defined in terms of static pressure:

$$P = p\left(1 + \frac{\gamma - 1}{2} M^2\right)^{\frac{\gamma}{\gamma-1}} \tag{A2}$$

$$q = \frac{\rho v^2}{2g_c} = \frac{p}{2g_c Rt} M^2 \gamma g_c Rt = \frac{1}{2} p\gamma M^2 \tag{A3}$$

Substituting equations (A2) and (A3) into equation (A1) yields

$$C_D = \frac{p_A\left(1 + \frac{\gamma - 1}{2} M_A^2\right)^{\frac{\gamma_A}{\gamma_A-1}} - p_B\left(1 + \frac{\gamma_B - 1}{2} M_B^2\right)^{\frac{\gamma_B}{\gamma_B-1}}}{\frac{1}{2} p_A \gamma_A M_A^2} \tag{A4}$$

Equation (A4), when solved for p_B, becomes equation (5), as shown in the Method of Analysis section:

$$p_B = p_A \frac{\left(1 + \frac{\gamma_A - 1}{2} M_A^2\right)^{\frac{\gamma_A}{\gamma_A-1}} - \frac{1}{2} \gamma_A M_A^2 C_D}{\left(1 + \frac{\gamma_B - 1}{2} M_B^2\right)^{\frac{\gamma_B}{\gamma_B-1}}} \tag{5}$$

Generally, since static-temperature and Mach number changes across the flame holder are not great, $\gamma_A \approx \gamma_B$, and $\left(1 + \dfrac{\gamma_A - 1}{2} M_A^2\right) \approx \left(1 + \dfrac{\gamma_B - 1}{2} M_B^2\right)$; thus equation (5) may be written more simply:

$$p_B \approx p_A \left[1 - \frac{\gamma_A M_A^2 C_D}{2\left(1 + \dfrac{\gamma_A - 1}{2} M_A^2\right)^{\frac{\gamma_A}{\gamma_A - 1}}} \right] \tag{A5}$$

Equation (6) in the Method of Analysis section is merely a statement of the continuity relation across the flame holder:

$$p_A A_A M_A \sqrt{\frac{\gamma_A g_c}{R_A t_A}} \approx p_B A_B M_B \sqrt{\frac{\gamma_B g_c}{R_B t_B}} \tag{A6}$$

Again, when static-temperature or Mach number changes are small across the flame holder, and when $A_A \approx A_B$, equation (6) or (A6) becomes

$$M_B \approx M_A \frac{p_A}{p_B} \tag{A7}$$

APPENDIX B

DERIVATION OF MIXING RELATION

Heat-balance equation. - For two streams A and B mixing to form a resultant stream C, an enthalpy balance with no losses requires

$$W_A c_A (t_A - t_{ref}) + W_B c_B (t_B - t_{ref}) = W_C c_C (t_C - t_{ref}) \qquad (B1)$$

where the specific heats are averaged between the stream temperatures and a reference temperature t_{ref}. If t_B is selected as the reference temperature, equation (B1) becomes

$$W_A c_A (t_A - t_B) = W_C c_C (t_C - t_B) \qquad (B2)$$

which when rearranged to solve for t_C gives equation (7) in the Method of Analysis section:

$$t_C = t_B + \frac{(t_A - t_B) c_A W_A}{W_C c_C} \qquad (7)$$

Continuity equation. - The usual mass-flow continuity equation for the mixing streams is written as:

$$W_A + W_B = W_C \qquad (B3)$$

This form is expanded by expressing the mass flow W as pAv/Rt and introducing the Mach number by the definition $v = M\sqrt{\gamma g_c Rt}$. Equation (B3) then becomes

$$p_A A_A M_A \sqrt{\frac{\gamma_A g_c}{R_A t_A}} + p_B A_B M_B \sqrt{\frac{\gamma_B g_c}{R_B t_B}} = p_C A_C M_C \sqrt{\frac{\gamma_C g_c}{R_C t_C}} \qquad (B4)$$

This is simplified by the requirement that the static pressure of the two mixing streams is equal; thus $p_A = p_B$. Equation (B4) can then be rearranged to the form of equation (8) in the Method of Analysis section.

$$p_C = p_B \frac{A_A M_A \sqrt{\frac{\gamma_A}{R_A t_A}} + A_B M_B \sqrt{\frac{\gamma_B}{R_B t_B}}}{A_C M_C \sqrt{\frac{\gamma_C}{R_C t_C}}} \qquad (8)$$

3042

 Dynamic momentum balance. - A dynamic momentum balance for two mixing streams, for the case in this analysis where the two mixing streams are at equal static pressures denoted by p_B, and $A_A + A_B = A_C$, is

$$W_A v_A + W_B v_B = W_C v_C + (A_A + A_B)(p_C - p_B) g_c \tag{B5}$$

From the substitutions of $W = \dfrac{pAv}{Rt}$ and $v^2 = M^2 \gamma g_c Rt$, equation (B5) becomes

$$p_A A_A \gamma_A g_c M_A^2 + p_B A_B \gamma_B g_c M_B^2 = p_C A_C \gamma_C g_c M_C^2 + (A_A + A_B)(p_C - p_B) g_c \tag{B6}$$

Rearranging and simplifying equation (6) and substituting $p_A = p_B$ yield

$$M_C^2 = \frac{p_B A_A \gamma_A M_A^2 + p_B A_B \gamma_B M_B^2 - (A_A + A_B)(p_C - p_B)}{p_C A_C \gamma_C} \tag{B7}$$

Finally, equation (B7) is put in the form of equation (9) of the Method of Analysis section by taking square roots and noting that $A_C = A_A + A_B$. Additional rearrangement yields

$$M_C = \sqrt{\left(\frac{p_B}{p_C}\right) \left[\frac{A_A(1 + \gamma_A M_A^2) + A_B(1 + \gamma_B M_B^2)}{A_C \gamma_C}\right] - \frac{1}{\gamma_C}} \tag{9}$$

APPENDIX C

DETAILS OF ANALYTICAL CALCULATIONS

The application of the simple operations discussed in the analysis of this report to the stepwise calculation of pressure and Mach number changes in divided- and nondivided-flow combustors is given in tables II and III. In table II are given the changes between stations in the analytical models (fig. 1) and the equations from the Method of Analysis section which are applicable for each change. Table III is a sample calculation for a divided-flow engine operated under the stated conditions given in the Conditions for Analysis section for 25-percent primary-zone air flow through a primary zone occupying 50 percent of the total combustor area with a flame-holder pressure-loss coefficient $\Delta P/q$ of 2. Table III also includes a sample calculation for a nondivided-flow engine operated at the same over-all temperature ratio as the divided-flow configuration.

The calculations for table III were performed by using the general equations (1) to (11) given in the text, with the equations written specifically for each station.

The analytical procedure illustrated herein is general and can be applied to any divided-flow system in which the combustor-inlet Mach number is 0.18, a usual order of magnitude for ram-jet combustors, and burning in the primary-zone area is stoichiometric. The selection of a specific free-stream Mach number affects only subsequent values of specific-heat ratios, which are of second-order importance.

REFERENCES

1. Cervenka, A. J., and Dangle, E. E.: Effect of Fuel-Air Distribution on Performance of a 16-Inch Ram-Jet Engine. NACA RM E52D08, 1952.

2. Cervenka, A. J., Bahr, D. W., and Dangle, E. E.: Effect of Fuel-Air Ratio Concentration in Combustion Zone on Combustion Performance of a 16-Inch Ram-Jet Engine. NACA RM E53B19, 1953.

3. Reynolds, Thaine W., and Ingebo, Robert D.: Combustion Efficiency of Homogeneous Fuel-Air Mixtures in a 5-Inch Ram-Jet-Type Combustor. NACA RM E52I23, 1952.

4. Ruegg, F. W., and Klug, H. J.: Analytical and Experimental Studies with Idealized Gas Turbine Combustors. Jour. Res. Nat. Bur. Standards, vol. 49, no. 5, 1952, pp. 279-298.

5. Shapiro, Ascher H., and Hawthorne, W. R.: The Mechanics and Thermodynamics of Steady One-Dimensional Gas Flow. Jour. Appl. Mech., vol. 14, no. 4, Dec. 1947, pp. A317-A336.

6. Keenan, Joseph H., and Kaye, Joseph: Gas Tables. John Wiley & Sons, Inc., 1948.

7. Cervenka, A. J., and Miller, R. C.: Effect of Inlet-Air Parameters on Combustion Limit and Flame Length in 8-Inch Diameter Ram-Jet Combustion Chamber. NACA RM E8C09, 1948.

3042

TABLE I. - SPECIFICATIONS AND ANALYSIS OF MIL-F-5624A GRADE JP-4

ENGINE FUEL

	Specifications	Analysis
A.S.T.M. distillation D86-46, °F		
Initial boiling point		140
Percentage evaporated		
5		199
10	250 (max)	224
20		250
30		270
40		290
50		305
60		325
70		352
80		384
90		427
Final boiling point	550 (max)	487
Residue, percent	1.5 (max)	1.2
Loss, percent	1.5 (max)	0
Specific gravity, 60°/60° F	0.826 to 0.747	0.765
Reid vapor pressure, lb/sq in.	2.0 (min), 3.0 (max)	2.7
Hydrogen-carbon ratio		0.169
Net heat of combustion, Btu/lb	18,400 (min)	18,700

3042

3042

TABLE II. - STEPWISE OPERATIONS IN ANALYTICAL ENGINE MODELS

(a) Divided-flow combustor

Station	Identity of station	Simple operation at station	Applicable equations
0-1	Supersonic portion of diffuser	Isentropic area change with diffuser-efficiency correction	(1),(2) corrected for diffuser efficiency
1a-2a	Subsonic portion of diffuser	Isentropic area change	(1),(2)
1b-2b	Subsonic portion of diffuser	Isentropic area change	(1),(2)
2a-3a	Primary-zone flame holder	Flame-holder loss	(5),(6) or (A5),(A7)
3a-4a	Primary combustion zone	Constant-area temperature change	(3),(4)
4a-5a	Primary-zone exit nozzle	Isentropic area change	(1),(2)
2b-4b	Secondary zone	No change	
4b-5b	Secondary-zone exit nozzle	Isentropic area change	(1),(2)
5a,5b-6	Mixing zone	Constant momentum mixing	(7),(8),(9)

(b) Nondivided-flow combustor

Station	Identity of station	Simple operation at station	Applicable equations
0-1	Supersonic portion of diffuser	Isentropic area change with diffuser-efficiency correction	(1),(2) corrected for diffuser efficiency
1-2	Subsonic portion of diffuser	Isentropic area change	(1),(2)
2-3	Flame holder	Flame-holder loss	(5),(6) or (A5),(A7)
3-6	Combustion zone	Constant-area temperature change	(3),(4)

TABLE III. - SAMPLE CALCULATION

(a) Divided-flow combustor

[25-Percent primary-zone air flow, 50-percent primary-zone
area, and flame-holder pressure-loss coefficient of 2]

Station	Value	Source
0-1	$M_0 = 3$	Given (see Conditions for Analysis section)
	$\eta_D = 0.65$	Given
	$\gamma_0 = 1.4$	Ref. 6
	$M_1 = 1$	Given (sonic throat)
	$A_0 = 1$	Arbitrary area value (total combustor area A_2 then is 1.2 as stated in the Conditions for Analysis section)
	$p_0 = 1$	Arbitrary pressure value (actual free-stream pressure values are not necessary and all further pressure values are expressed on this basis)
	$\gamma_1 = 1.375$	Ref. 6 (same value is used at stations 2a, 3a, 2b, 5b)
	$A_1 = 0.363$	Eq. (1) solved for A_1 (theoretical value of A_1 shown at left corrected for diffuser efficiency)
	$A_{1a} = 0.091$	A_{1a} is percent primary-zone air flow times A_1
	$A_{1b} = 0.272$	A_{1b} is percent seondary-zone air flow times A_1
	$P_0 = 36.7$	Eq. (10)
	$p_1 = 12.6$	Eq. (2) with value of p_1 from equation multiplied by 0.65 to correct for diffuser efficiency
	$P_1 = 23.8$	Eq. (10) ($P_1 = 0.65 P_0$)
1a-2a	$A_{2a} = 0.60$	Assigned value (since total combustor area is taken as 1.2, this amounts to 50 percent of combustor area)
	$M_{2a} = 0.088$	Eq. (1) solved for M_{2a}
	$p_{2a} = 23.6$	Eq. (2)
	$P_{2a} = 23.8$	No change in total pressure for isentropic area change
1b-2b	$A_{2b} = 0.60$	Assigned value
	$M_{2b} = 0.276$	Eq. (1) solved for M_{2b}
	$p_{2b} = 22.5$	Eq. (2)
	$P_{2b} = 23.8$	No change in total pressure for isentropic change

3042

TABLE III. - Continued.   SAMPLE CALCULATION

(a) Continued.   Divided-flow combustor

[25-Percent primary-zone air flow, 50-percent primary-zone
area, and flame-holder pressure-loss coefficient of 2]

Station	Value	Source
2a-3a	$C_D = 2$	Assigned value
	$p_{3a} = 23.4$	Eq. (5) or (A5)
	$M_{3a} = 0.089$	Eq. (6) or (A7)
	$P_{3a} = 23.5$	Eq. (10)
3a-4a	$\tau = 4.05$	Given (see Conditions for Analysis section)
	$\gamma_{4a} = 1.245$	Ref. 6 (the same value is used at station 5a)
	$M_{4a} = 0.190$	Eq. (3) solved for M_{4a} $(\tau = T_{4a}/T_0 = T_{4a}/T_{3a})$
	$p_{4a} = 21.4$	Eq. (4)
	$P_{4a} = 21.8$	Eq. (10)
4a-5a, 2b-5b	$M_{5a} = 0.151$ $M_{5b} = 0.383$ $A_{5a} = 0.75$ $A_{5b} = 0.45$ $p_{5a} = p_{5b} = 21.5$	At stations 5a and 5b there is an area change to fulfill the conditions: $p_{5a} = p_{5b}$, and $A_{5a} + A_{5b} = A_{2a} + A_{2b}$ as over-all combustor area remains the same. Values of p_{5a} and p_{5b} may be written in terms of p_{4a} and p_{4b} (P_{2b}), respectively, by eq. (2). Values of A_{5a} and A_{5b} may be written in terms of A_{4a} and A_{4b} $(A_{2a}$ and $A_{2b})$, respectively, by eq. (1). By a simultaneous solution of these four equations and the two pressure and area requirements, M_{5a}, M_{5b}, p_{5a}, p_{5b}, A_{5a}, and A_{5b} are found.
	$P_{5a} = 21.8$ $P_{5b} = 23.8$	No change in total pressure for isentropic area change
5-6	$T_0 = 1100^{\circ}$ R	Given
	$T_{5a} = 4460^{\circ}$ R	Given $(T_{5a} = T_0 \tau)$

TABLE III. - Continued.   SAMPLE CALCULATION

(a) Concluded.   Divided-flow combustor

[25-Percent primary-zone air flow, 50-percent primary-zone
area, and flame-holder pressure-loss coefficient of 2]

Station	Value	Source
5-6	$t_{5a} = 4448^{\circ}$ R	Eq. (11)
	$t_{5b} = 1071^{\circ}$ R	Eq. (11) $(T_{5b} = T_0)$
	$W_{5a}/W_6 = 0.262$	Original primary-stream fraction of 0.25 corrected for the additional 0.067 fuel-air ratio of injected fuel
	$c_{5a} = 0.312$ Btu/lb $^{\circ}$R	Stoichiometric combustion of a fuel with a 0.167 hydrogen-carbon weight ratio yields a product consisting of 19.9 weight percent CO_2, 8.1 percent H_2O, and 72.0 percent N_2. From ref. 6, average specific heat of this product may be calculated for temperature range from 1071° to 4448° R.
	$c_6 = 0.286$ Btu/lb $^{\circ}$R	Specific heat from ref. 6 (an average value over range from 1071° to 2036° R)
	$t_6 = 2036^{\circ}$ R	Eq. (7)
	$R_{5a}, R_{5b},$ $R_6 = 53.4$ ft-lb/lb $^{\circ}$R	Carbon-dioxide - water ratio of stoichiometric combustion products is such that combined molecular weight of products is 28.9, same as that of air. Thus gas constant of all streams is $1543/28.9 = 53.4$
	$A_6 = 1.2$	Total cross section remains constant
	$\gamma_6 = 1.314$	Ref. 6
	$p_6 = 21.5$	Eq. (8)
	$M_6 = 0.263$	Eq. (9)(eqs. (8) and (9) must be solved simultaneously)
	$P_6 = 22.5$	Eq. (10)
0-6	$P_6/P_0 = 0.613$	$P_0 = 36.7$. Most of pressure drop occurs in supersonic diffuser. If diffuser efficiency were 100 percent, then $P_6/P_0 = 0.613/0.65 = 0.943$.

TABLE III. - Concluded.   SAMPLE CALCULATION

(b) Nondivided-flow combustor

[Flame-holder pressure-loss coefficient of 2 with same total-
temperature ratio as corresponding divided-flow combustor]

| Station	Value	Source
0-1	$M_0 = 3$ $\eta_D = 0.65$ $\gamma_0 = 1.4$ $M_1 = 1$ $A_0 = 1$ $p_0 = 1$ $A_1 = 0.363$ $P_0 = 36.7$ $p_1 = 12.6$ $P_1 = 23.8$	Same values as in (a)
1-2	$A_2 = 1.2$	Given
	$\gamma_{2a} = \gamma_{3a} = 1.375$	Ref. 6
	$M_2 = 0.179$	Eq. (1) solved for M_2
	$p_2 = 23.2$	Eq. (2)
	$P_2 = 23.8$	No change in total pressure
2-3	$C_D = 2$	Assigned value
	$p_3 = 22.1$	Eq. (5) or (A5)
	$M_3 = 0.187$	Eq. (6) or (A7)
	$P_3 = 22.6$	Eq. (10)
3-6	$\tau = 1.875$	This corresponds to over-all temperature ratio in (a): $T_6/T_0 = 2060/1100 = 1.875$. T_6 is found from t_6 by eq. (11)
	$\gamma_6 = 1.325$	Ref. 6
	$M_6 = 0.271$	Eq. (3) solved for M_6
	$p_6 = 20.7$	Eq. (4)
	$P_6 = 21.7$	Eq. (10)
0-6	$P_6/P_0 = 0.591$	$P_0 = 36.7$. If supersonic diffuser efficiency were 100 percent, then $P_6/P_0 = 0.909$.
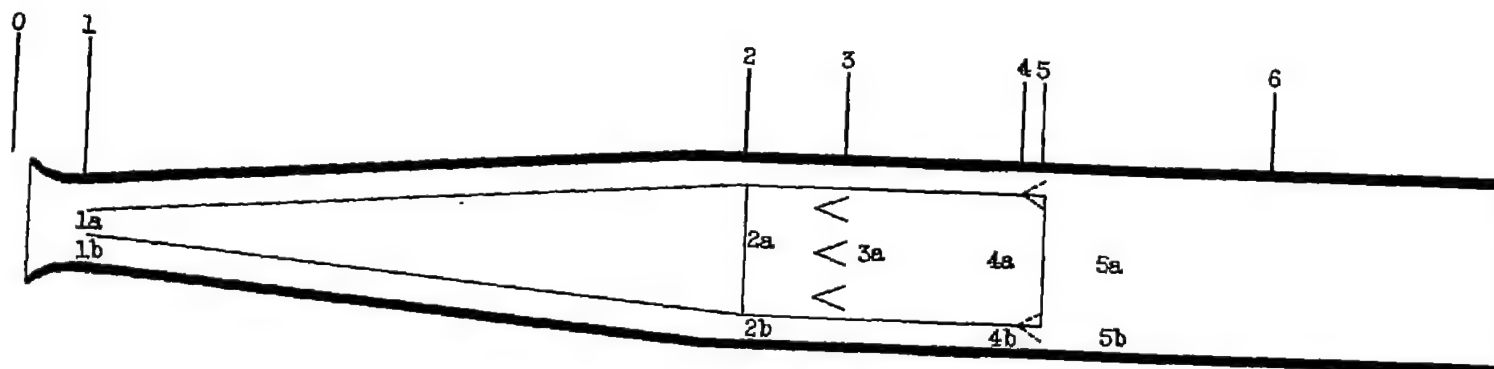
(a) Divided flow.
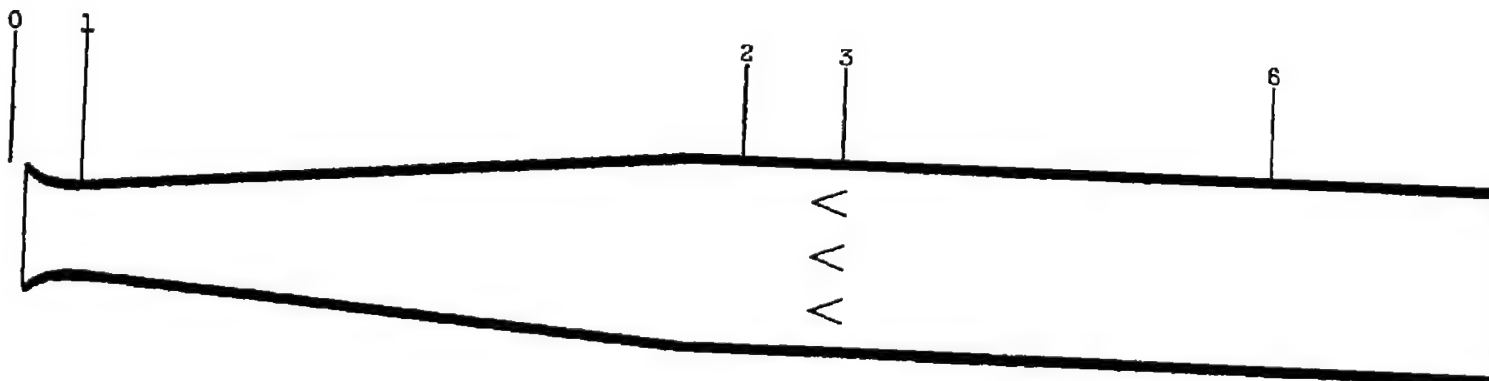
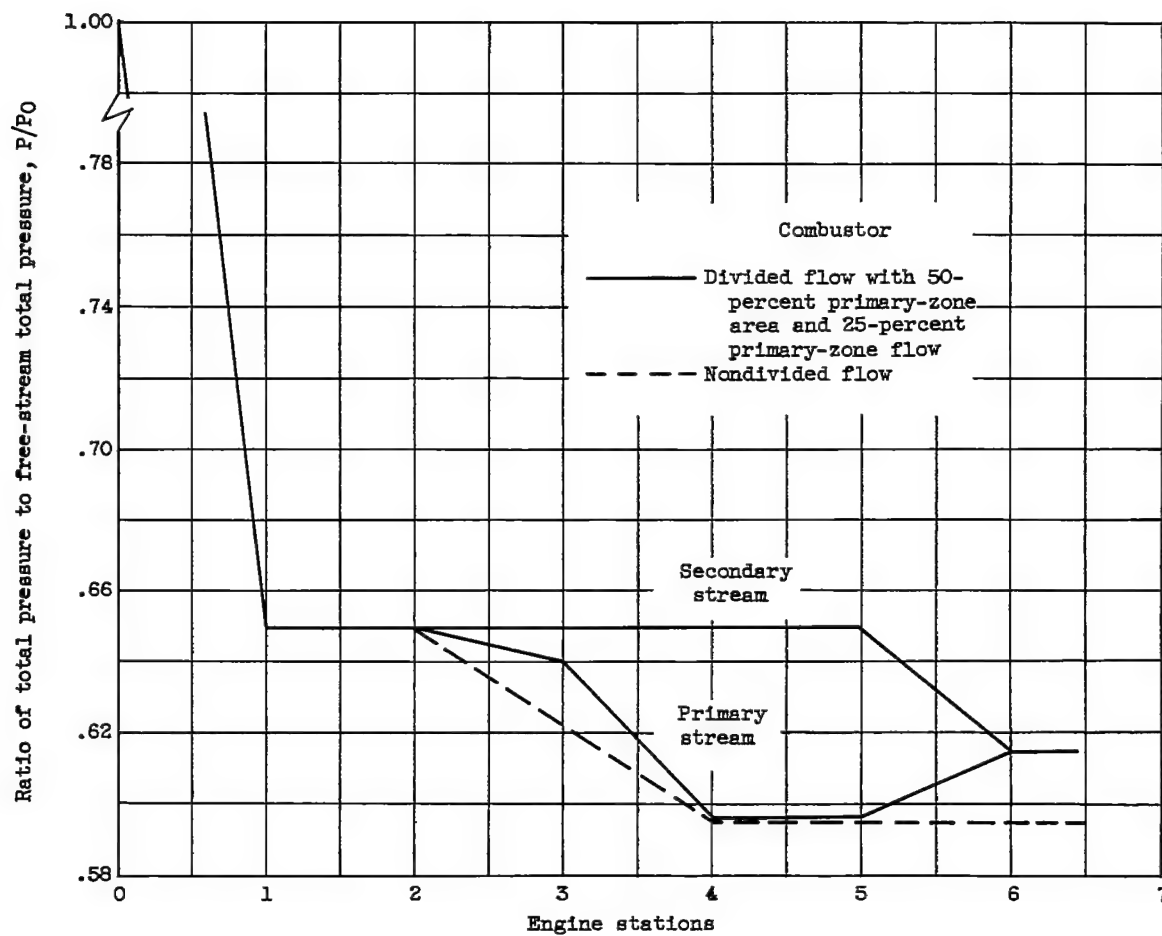(b) Nondivided flow.

CD-3315

Figure 1. - Analytical engine models.

3042

Figure 2. - Variations in total-pressure ratio through analytical model engine. Free-stream Mach number, 3.0; diffuser efficiency, 65 percent; combustor-inlet Mach number, 0.18; over-all combustor total-temperature ratio, 1.875.
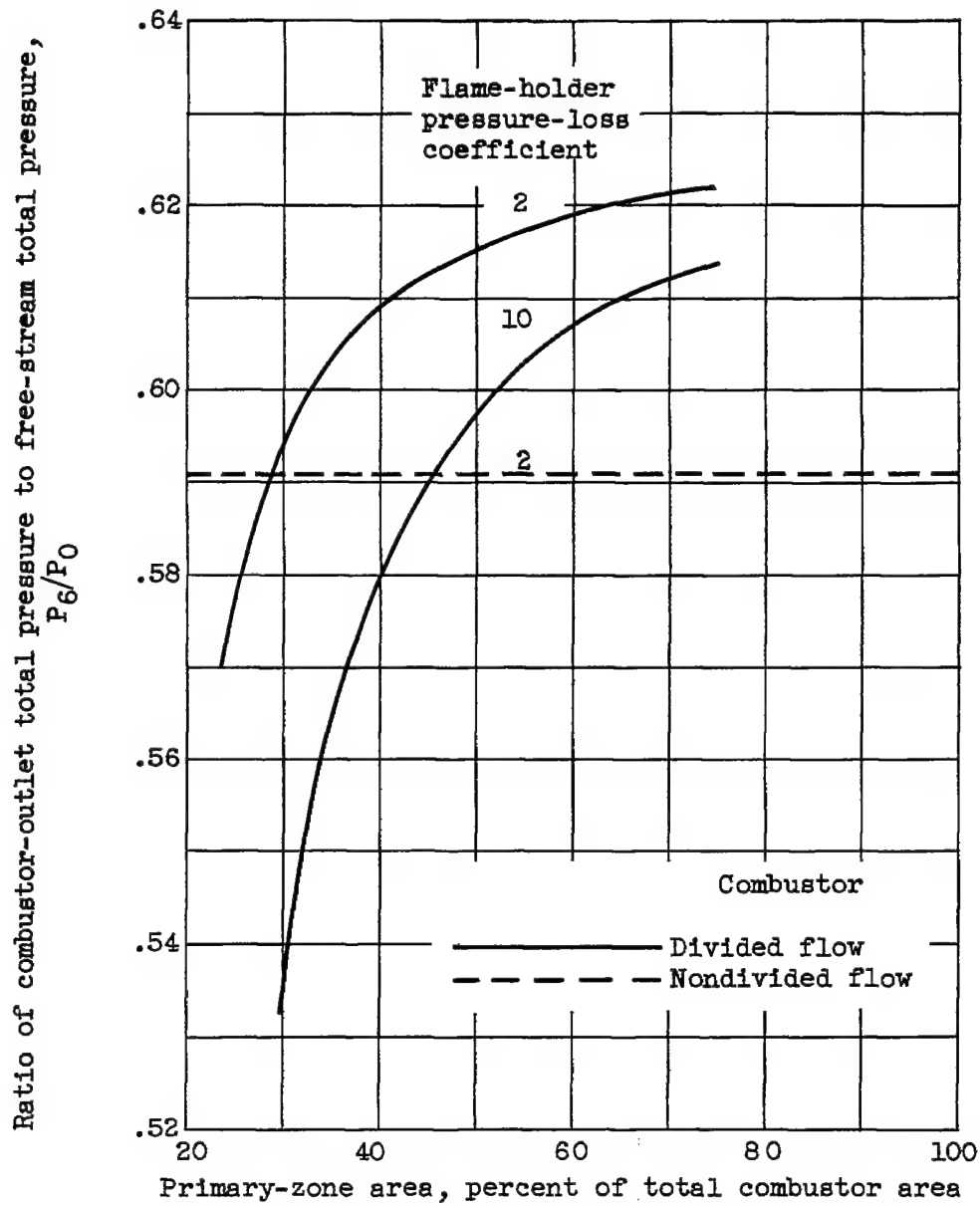
CONFIDENTIAL

Figure 3. - Effect of size of primary combustor
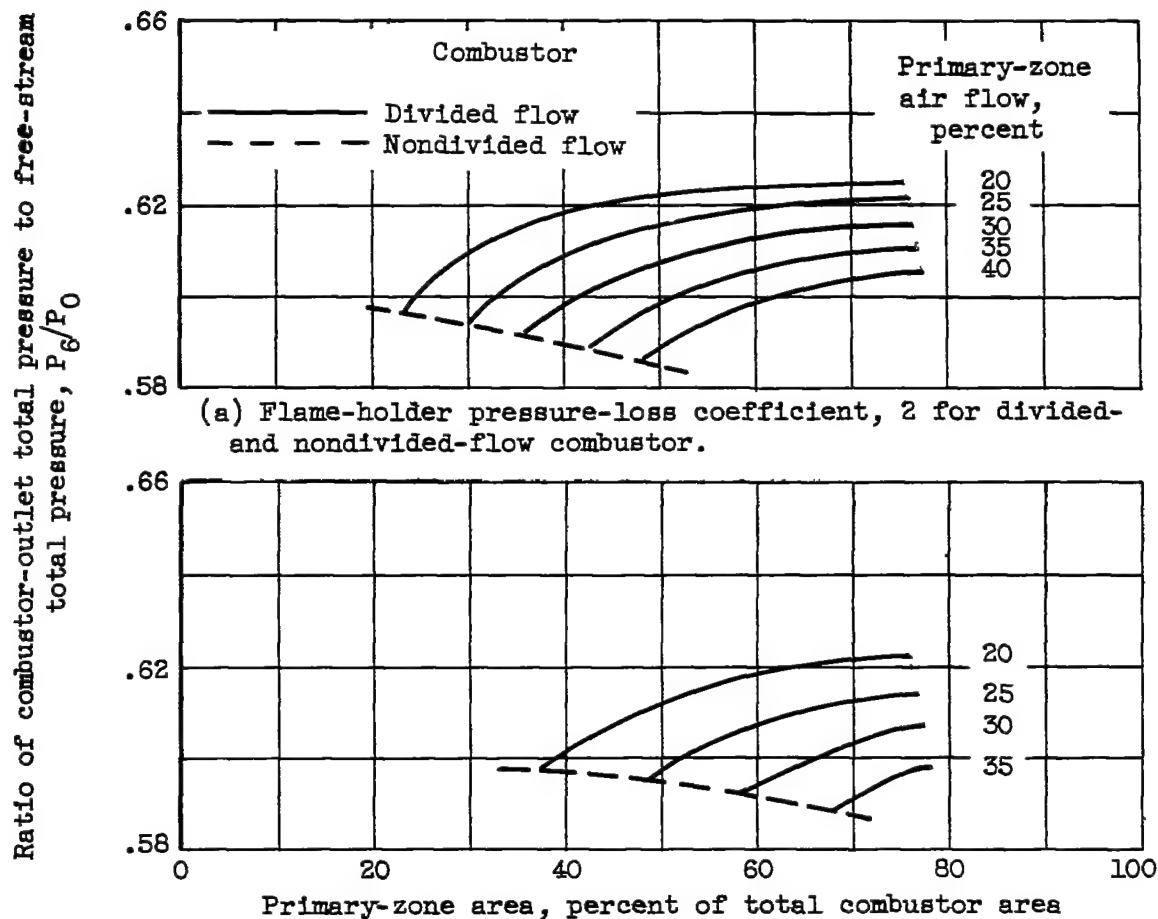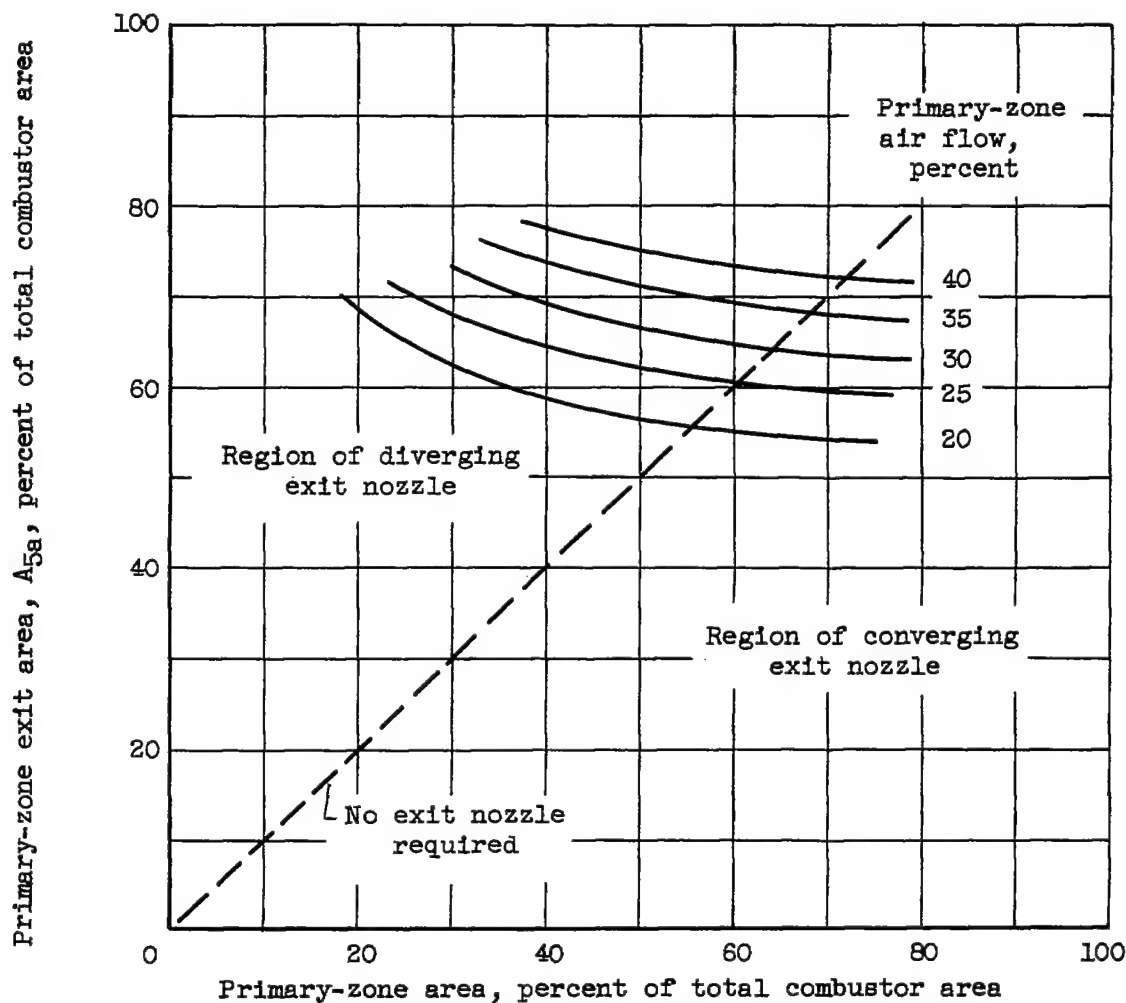area upon over-all pressure recovery. Over-all
fuel-air ratio, 0.017.

3042

(a) Flame-holder pressure-loss coefficient, 2 for divided- and nondivided-flow combustor.

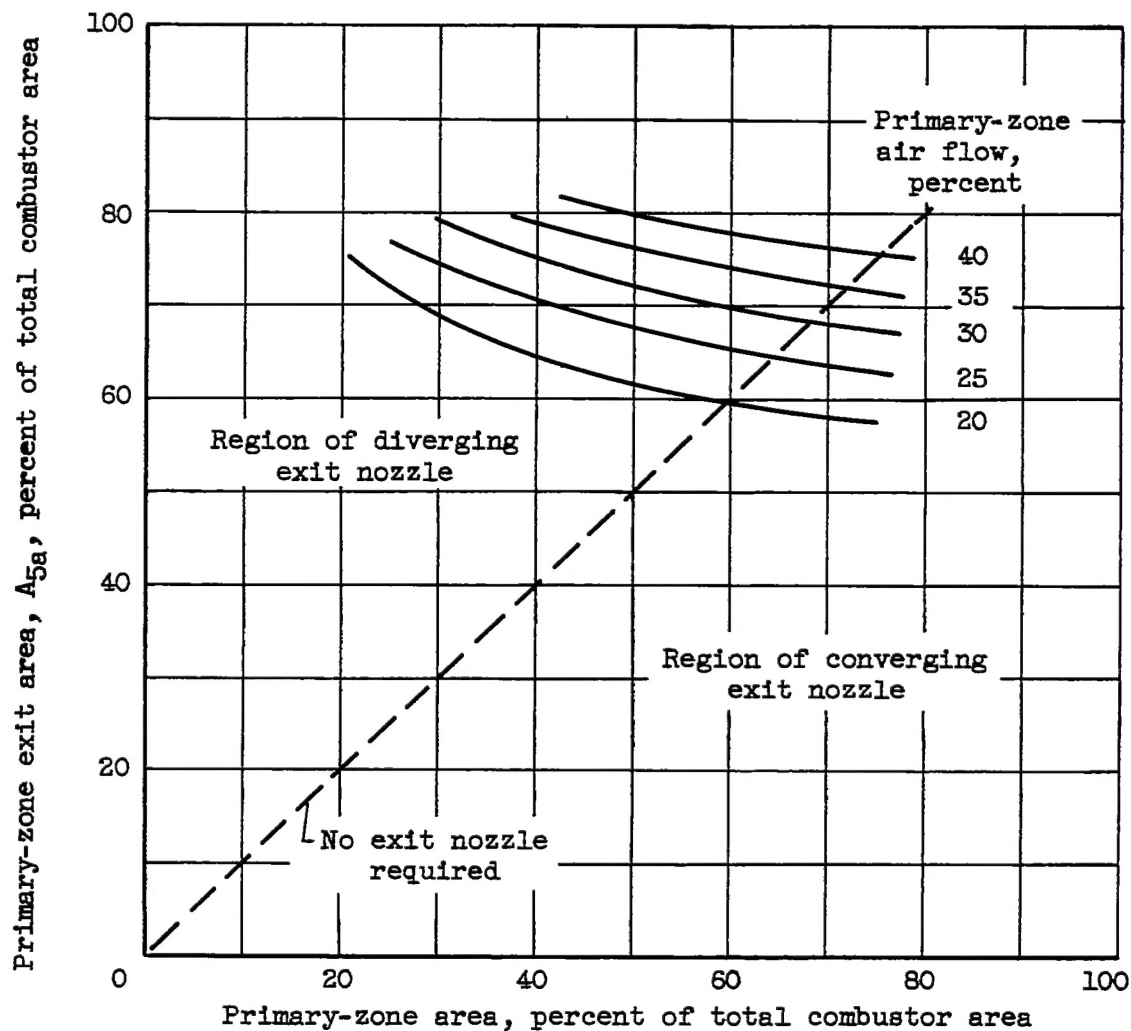(b) Flame-holder pressure-loss coefficient, 10 for divided-flow combustor and 2 for nondivided-flow combustor.

Figure 4. - Comparison of total-pressure ratios for several primary-zone air flows, and comparison of total-pressure ratios for divided- and nondivided-flow combustors for similar total-temperature ratios across combustors.

(a) Flame-holder pressure-loss coefficient, 2.

Figure 5. - Nozzle area at station 5 required to maintain
equal static pressures at stations 5a and 5b for several
primary-zone air flows.

3042

(b) Flame-holder pressure-loss coefficient, 10.

Figure 5. - Concluded. Nozzle area at station 5 required to
maintain equal static pressures at stations 5a and 5b for
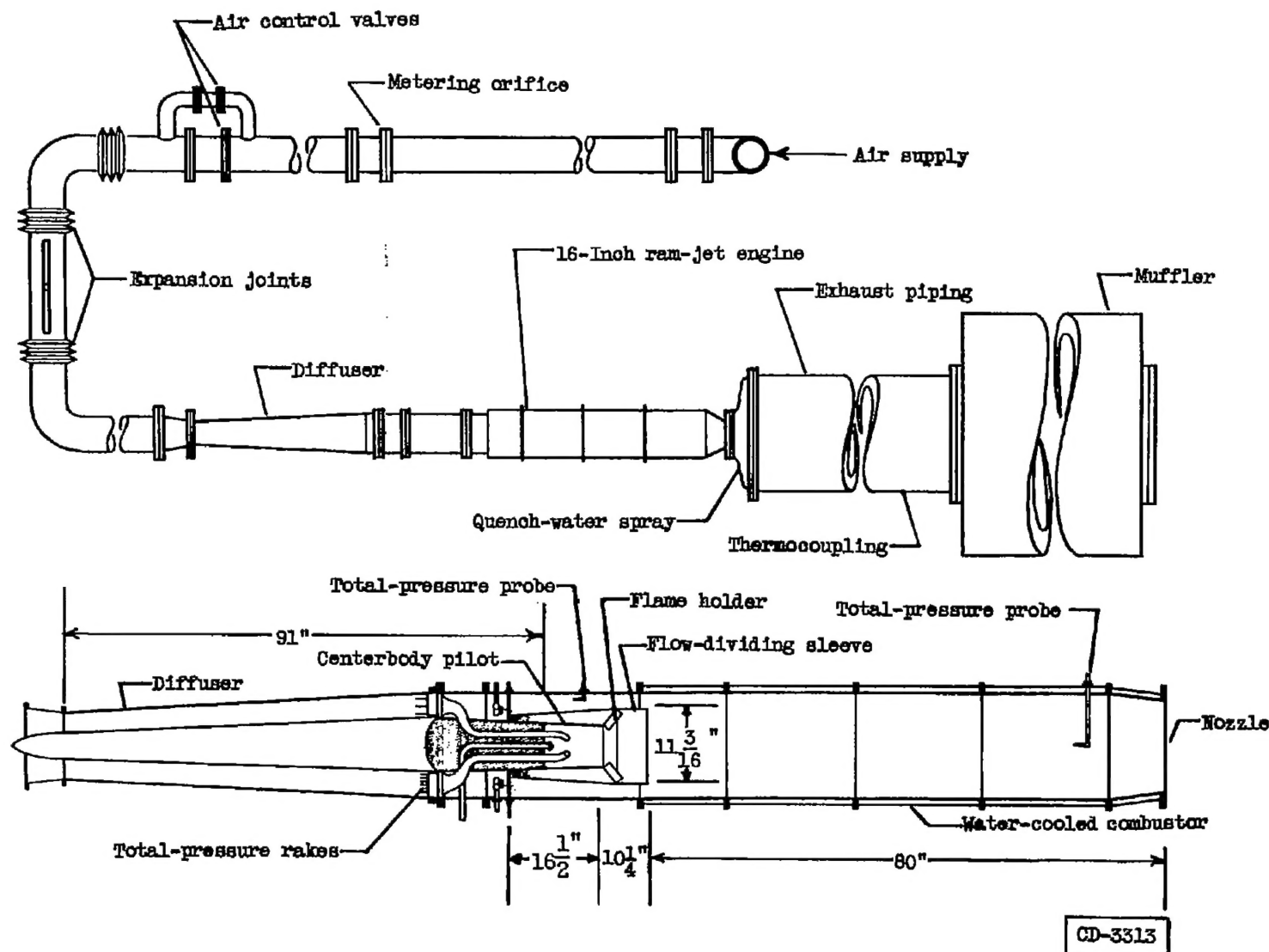several primary-zone air flows.

Figure 6. - Installation and dimensions of 16-inch ram-jet engine with flow-dividing sleeve.
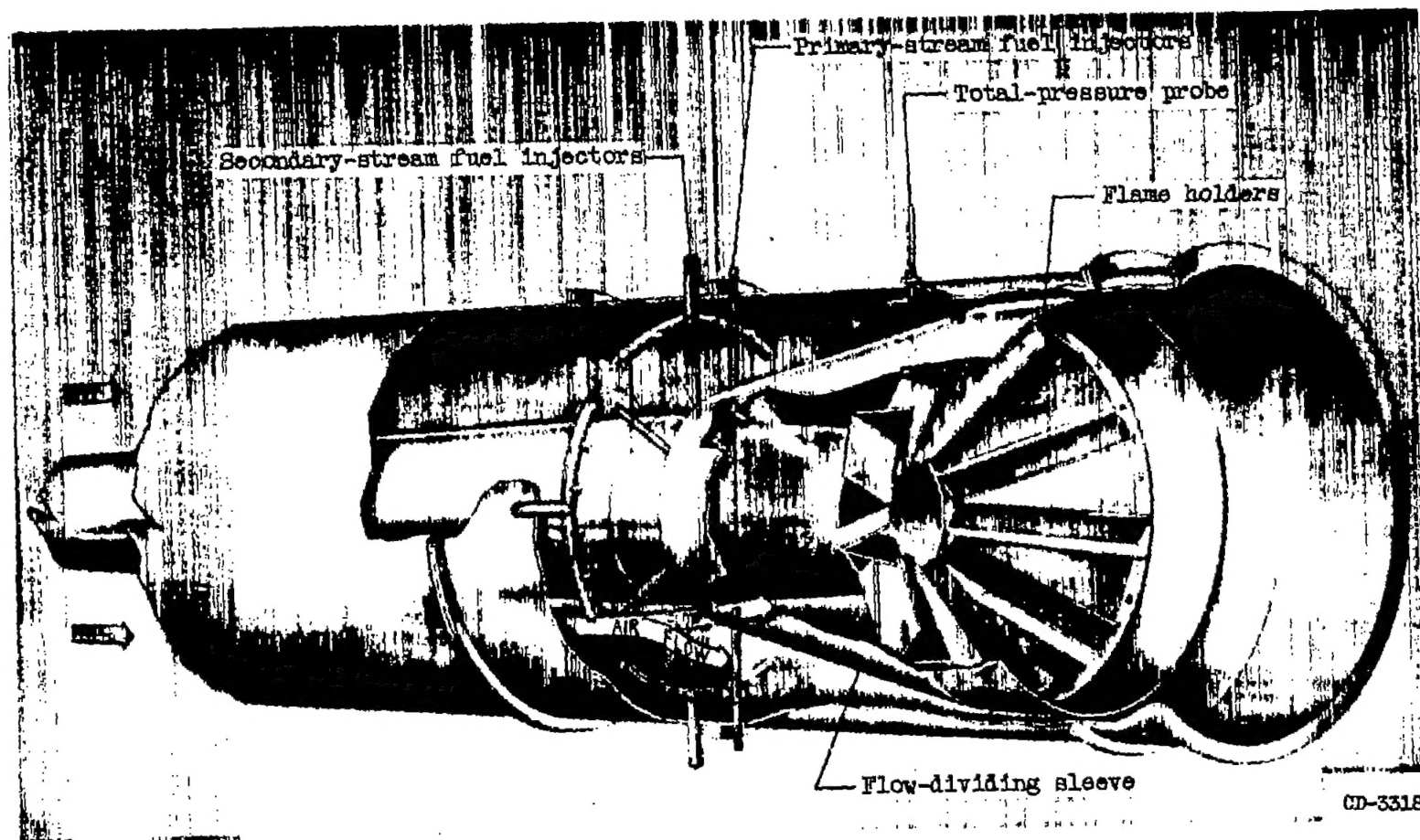
CD-3313

Secondary-stream fuel injectors

Primary-stream fuel injectors

Total-pressure probe

Flame holders

AIR

Flow-dividing sleeve

CD-3318

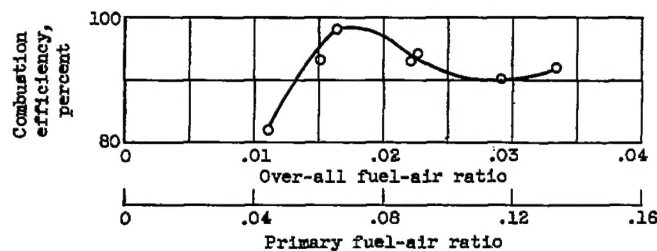Figure 7. - Divided-flow combustor showing view of flame holders.

CONFIDENTIAL

Figure 8. - Effect of primary and over-all fuel-
air ratio upon combustion efficiency of divided-
flow combustor with 50-percent primary-zone area
and 25-percent primary-zone air flow.

Divided-flow combustor

 o Primary-stream fuel injection (fig. 8)
 □ Primary- and secondary-stream fuel
    injection (primary at 0.067)
 ◊ Primary- and secondary-stream fuel
    injection (primary at 0.092)
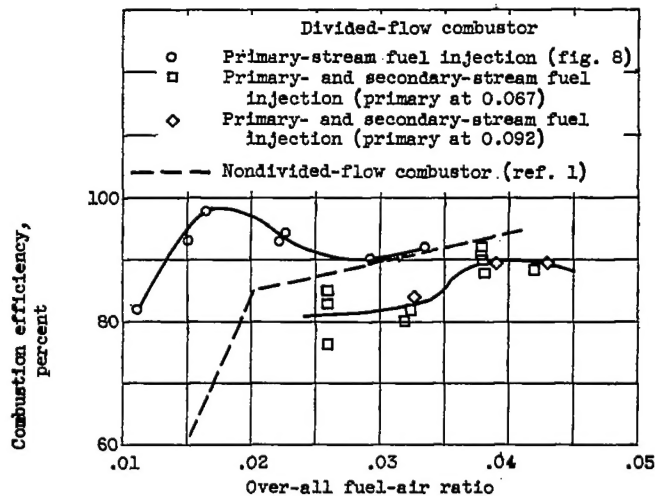
 — — Nondivided-flow combustor (ref. 1)

Figure 9. - Comparison of combustion efficiency
of divided-flow combustor, with and without
secondary-stream fuel injection, with combus-
tion efficiency of nondivided-flow combustor.

Divided-flow combustor

 o Primary-stream fuel injection
 □ Primary- and secondary-stream
    fuel injection (primary
    at 0.067)
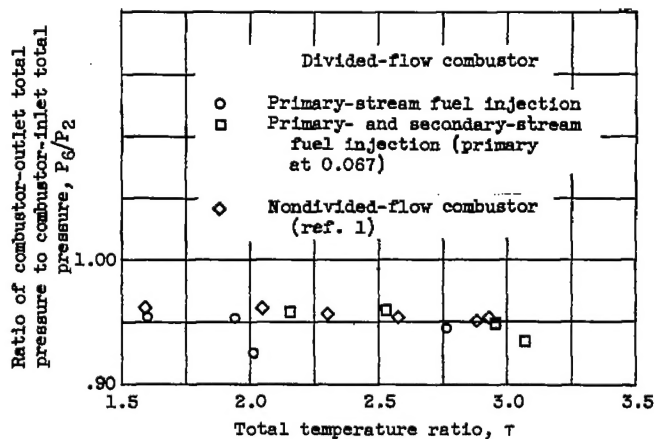
 ◊ Nondivided-flow combustor
    (ref. 1)

Figure 10. - Comparison of total-pressure ratio
of divided-flow combustor, with and without
secondary-stream fuel injection, with total-
pressure ratio of nondivided-flow combustor.

CONFIDENTIAL